Available online at www.sciencedirect.com
SCIENCE DIRECT
Journal of Sound and Vibration 295 (2006) 781–796
JOURNAL OF SOUND AND VIBRATION
www.elsevier.com/locate/jsvi

Experimental determination of the tonal noise sources in a centrifugal fan

Sandra Velarde-Suárez, Rafael Ballesteros-Tajadura*, Juan Pablo Hurtado-Cruz, Carlos Santolaria-Morros

Universidad de Oviedo. Área de Mecánica de Fluidos, Campus de Gijón, 33271 Gijón, Spain

Received 21 February 2005; received in revised form 20 December 2005; accepted 24 January 2006
Available online 11 April 2006

Abstract

In this work, an experimental study about the aerodynamic tonal noise sources in a centrifugal fan with backward-curved blades has been carried out. Acoustic pressure measurements at the fan exit duct and pressure fluctuation measurements on the volute surface have been made for different flow rates. A correlation study of both pressure signals has been made in order to explain some of the features of the aerodynamic tonal noise generation. A strong source of noise caused by the interaction between the fluctuating flow leaving the impeller and the volute tongue is appreciated. The unsteady forces exerted on the fan blades constitute another noise generation mechanism, which affects the whole extension of the impeller, thus transmitting pressure fluctuations to the entire volute casing. The relative importance of this mechanism compared to the impeller–tongue interaction depends on the flow rate.
© 2006 Elsevier Ltd. All rights reserved.

1. Introduction

Most of the current studies on aerodynamic noise of turbulent flows are based on the acoustic analogy [1]. This theory considers the flow field as a superposition of a small amplitude fluctuating sound field and a non-perturbed aerodynamic field that generates the fluctuating field. Powell's theory of vortex sound [2] is an alternative to Lighthill's analogy, which expresses noise generation as a function of velocity and vorticity fields.

The acoustic analogy has been used for a long time just as a dimensional analysis tool due to the difficulty and the high cost of numerical simulations of turbulent three-dimensional (3-D) flows. Nowadays, the development of powerful computers and more efficient codes has concentrated the interest on the acoustic analogy; thus, it is possible to obtain the noise generation based upon the unsteady incompressible description of the flow acting as a source term of the acoustic pressure field. Once the source term has been determined by means of the flow field, Lighthill's equation can be solved using the normalized Green function method.

Ffowcs Williams and Hawkings [3] applied the acoustic analogy to a flow field with solid surfaces in arbitrary motion and derived a wave equation in which some terms are identified with the different

*Corresponding author. Fax: +34 985182098.
E-mail address: rballest@uniovi.es (R. Ballesteros-Tajadura).

0022-460X/$ - see front matter © 2006 Elsevier Ltd. All rights reserved.
doi:10.1016/j.jsv.2006.01.049

Nomenclature

B	volute width (mm)
BEP	best efficiency point
BPF	blade passing frequency
CPS (f)	coherent power spectrum of volute pressure fluctuations (Pa)
$CPSL_{BPF}$	coherent power spectrum level at the BPF (dB, Ref. 20 μPa)
CPS_{BPF}	amplitude (rms) of coherent power spectrum at the BPF (Pa)
D	diameter (mm)
f	frequency (Hz)
P_T	total pressure rise (Pa)
p	acoustic pressure (Pa)
p_0	reference acoustic pressure (20 μPa)
PS	power spectrum of volute pressure fluctuations (Pa)
Q	flow rate (m^3/s)
L_P	sound pressure level, $L_P = 20\log p/p_0$ (dB, Ref. 20 μPa)
L_W	overall sound power level (dB, Ref. 10^{-12} W)
γ^2	coherence function between volute pressure fluctuations and sound pressure levels at the fan exit duct
Ψ	total pressure coefficient, $\Psi = P_T/\rho\Omega^2D^2$
φ	flow coefficient, $\varphi = Q/\Omega D^3$
ρ	density (kg/m^3)
Ω	rotational frequency (rad/s)

aeroacoustic generation mechanisms: quadrupolar noise, related with turbulence shear stresses; dipolar noise, produced by steady and unsteady forces exerted by the moving surfaces on the flow; and monopolar or thickness noise, due to the volume displacement of the moving surfaces. Among the above-mentioned mechanisms, the main contribution to the noise generated by fans is due to the forces acting on the blades, vanes and casing, produced by their interaction with the turbulent flow [4]. In the particular case of centrifugal fans, many authors have studied the pressure fluctuations at the volute tongue, due to the interaction between the non-uniform impeller flow and the fixed volute, as an important source of aerodynamic tonal noise generation in centrifugal machinery (see, for example, [5–7]). According to these investigations, the location of the effective noise source is restricted to the vicinity of the volute tongue, and the extension of the effective source region could be determined by a correlation analysis between the acoustic pressure radiated by the fan and the pressure fluctuation on the volute surface.

The possibility of confining the aerodynamic generation of tonal noise to a specific region of the flow field is of great interest in order to simplify the resolution of the acoustic analogy equations and to be able to predict the fan tonal noise generation. Thompson and Hourigan [8] made a prediction of the blade passing tone of a centrifugal fan by solving Powell's wave equation using a finite-element method. The acoustic forcing term was derived from experimental velocity data obtained by Shepherd and Lafontaine [9] using a particle image velocimetry (PIV) method. In these interesting works, the authors considered that the tonal noise generation was restricted to a rectangular area near the volute tongue, in which the velocity data were determined.

A survey of the literature shows examples where surface pressure measurements have been applied successfully in both centrifugal and axial fan noise research. Carolus and Stremel [10] have exposed some of these examples and their own application to a low-pressure axial fan, thus analyzing the contribution of the inlet turbulence to the generation of noise.

In this work, an experimental study about the aerodynamic tonal noise sources in an industrial centrifugal fan with backward-curved blades has been carried out. Acoustic pressure measurements at the fan exit duct and pressure fluctuation measurements on the volute surface (especially in the vicinity of the volute tongue) have been made at different flow rates. The correlation between both pressure signals leads to determine the main noise generation mechanisms and the zone of effective acoustic radiation. The study is focused on the fundamental blade passing frequency (BPF), analyzing the influence of the flow rate.

2. Experimental setup

The machine tested is a simple aspirating centrifugal fan driven by an AC 9.2 kW motor rotating at 1500 rev/min, with a fluctuation level lower than 0.5% for the whole range of the analyzed flow rates. The

shrouded rotor tested has 10 backward-curved blades with an outlet diameter of 400 mm. The blades are made of flat sheet metal. The minimum distance between the impeller and the volute tongue is 12.5% of the outlet impeller diameter. The widths of the impeller and volute are, respectively, 130 and 248 mm. Fig. 1 shows two photographs of the fan tested and Table 1 summarizes the main dimensions of the impeller tested.

The tests for the aerodynamic and acoustic characterization of the fan have been carried out in a standardized ducted installation (type B according to ISO 5136 [11]). Fig. 2 shows a drawing of this test installation. More details about the installation and procedures have been reported in previous works [12,13]. After leaving the fan, air flows through a straightener in order to remove the swirl generated by the fan; the measurement instruments were placed at sections A (static pressure) and B (flow rate and sound pressure level). At the end of the facility, an anechoic termination removes undesired noise reflections and the regulation cone permits to modify the fan operating point. The following maximum uncertainties were established for the measured and calculated magnitudes:

$$\text{Total pressure} : \pm 1.4\% \ (\pm 8\,\text{Pa}),$$
$$\text{Flow rate} : \pm 2\% \ (\pm 0.03\,\text{m}^3/\text{s}),$$
$$\text{Shaft power} : \pm 2\% \ (\pm 40\,\text{W}).$$

In Figs. 3 and 4, the total pressure rise, efficiency and overall sound power level have been represented as a function of flow rate. The best efficiency point (BEP) corresponds to a flow rate $Q = 0.92\,\text{m}^3/\text{s}$, with a total pressure rise $P_T = 500\,\text{Pa}$ and total efficiency of 0.77. The overall sound power level (L_W) presents its minimum values close to the BEP.

In Fig. 5, the total pressure coefficient Ψ has been represented as a function of the flow coefficient φ. The flow rates selected for this experimental study have been represented by white squares. The BEP corresponds to a flow coefficient $\varphi = 0.093$, with a total pressure coefficient $\Psi = 0.105$.

Acoustic pressure measurements at the fan exit duct have been made using a B&K 4189 1/2″ microphone protected with a nose cone. Additionally, B&K 4138 1/8″ microphones were flush-mounted on the volute surface, especially in the vicinity of the volute tongue, in order to measure the surface pressure fluctuations. The uncertainty of these two types of microphones has been established by the manufacturer in $\pm 0.2\,\text{dB}$, with a confidence level of 95%. The signals from the microphones were introduced into a personal computer by means of an analog-to-digital card. The data acquisition frequency was chosen equal to 10 kHz per channel in

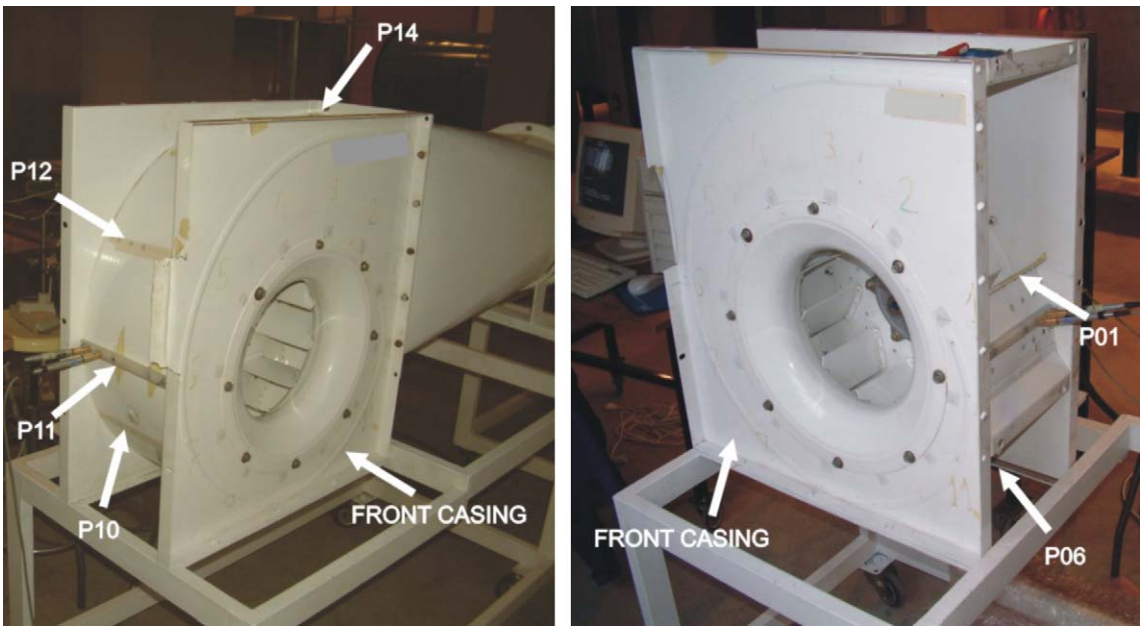

Fig. 1. Fan tested with the location of some measurement points.

Table 1
Impeller dimensions

Outlet diameter, D_e (mm)	400
Inlet diameter, D_i (mm)	280
Outlet width (mm)	130
Impeller–tongue distance (mm)	50
Impeller–tongue distance (% of outlet diameter)	12.5

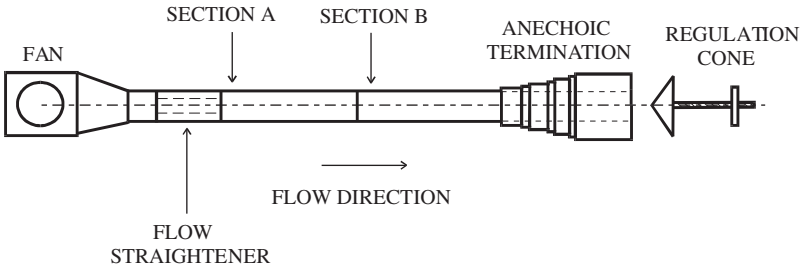

Fig. 2. Sketch of the test installation.

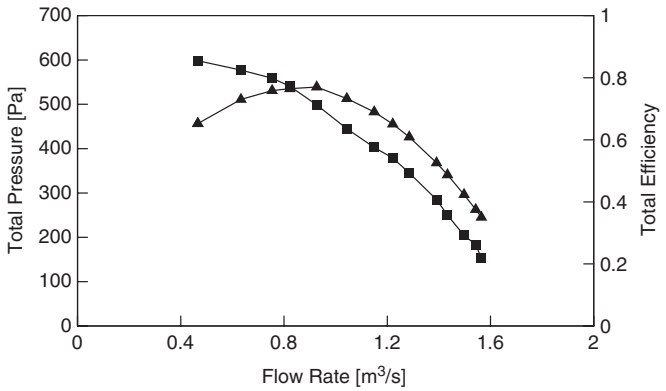

Fig. 3. Evolution of total pressure in Pa (black squares) and total efficiency (black triangles) with flow rate in m^3/s.

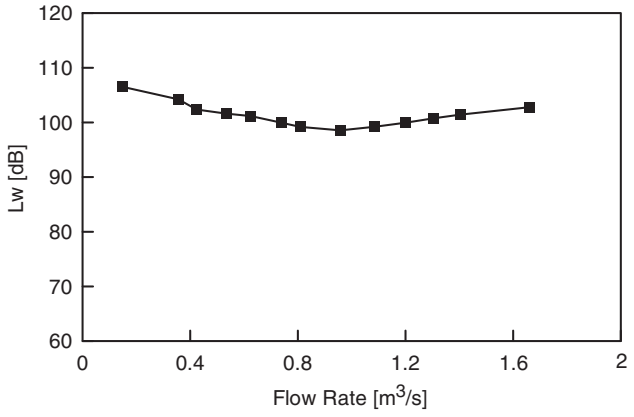

Fig. 4. Evolution of sound power level (dB, Ref. 10^{-12} W) with flow rate (m^3/s).

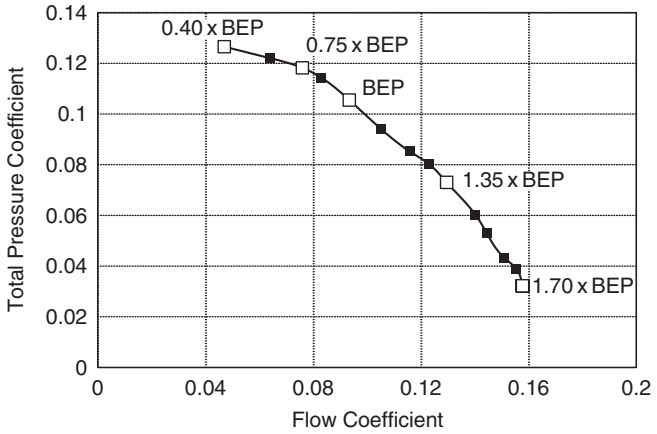

Fig. 5. Fan performance dimensionless curve (black squares) with the operating points selected in this study (white squares).

order to obtain a good resolution. Then, a fast Fourier transform (FFT) algorithm was used to obtain the power spectra of the pressure signals obtained both at the fan exit duct and at the volute surface.

3. Results and discussion

3.1. Acoustic pressures at the fan exit duct

Fig. 6 shows the power spectra of the sound pressure level (L_P) measured at the fan exit duct, for five different flow rates, represented by white squares in Fig. 5. They have been referred to the BEP: $0.40 \times$ BEP, $0.75 \times$ BEP, BEP, $1.35 \times$ BEP and $1.70 \times$ BEP.

Great broad band levels at low frequencies appear in these five spectra. A similar behavior were noticed in some previous works [12,13], carried out on a fan with the same volute as in the present case, driven by the same motor but with a forward curved blades impeller. Fehse and Neise [14] have investigated the generation of low-frequency noise in centrifugal fans. They found that the broad band components at low frequencies are generated by classical flow separation regions located on the impeller shroud and the blades suction sides.

In this work, we have focused the attention especially on the aerodynamic tonal noise at the BPF. In Fig. 7 the amplitudes of the main tonal noise components observed in Fig. 4 have been represented against the flow rate.

The peak at the BPF (250 Hz for this fan) appears clearly in all these flow rates. This component increases with the flow rate until $1.35 \times$ BEP, where a maximum amplitude of 98.5 dB is shown. Above this operating point the BPF decreases slightly. The first harmonic at 500 Hz increases with the flow rate over all the operating range, but its values are very low; in some cases (flow rates below the BEP), it is practically masked by the broad band noise at adjacent frequencies.

There is a peak at 275 Hz clearly shown with the same amplitude (about 85 dB) in all the operating points. Peaks at 300 and 325 Hz also appear, with slight variations depending on the flow rate. We must ascribe these levels at 275, 300 and 325 Hz to mechanical sources of noise; more explanation about these features will be added in the following sections.

3.2. Pressure fluctuations at the volute surface

Pressure fluctuation measurements have been made at five locations (P01–P05) very close to the volute tongue and at another nine locations (P06–P14) evenly distributed around the volute. Table 2 summarizes the angular coordinates of the measurement positions over the volute surface. Fig. 8 shows two sketches of the fan with the locations of the measurement points. Some of these measurement positions have been also marked in

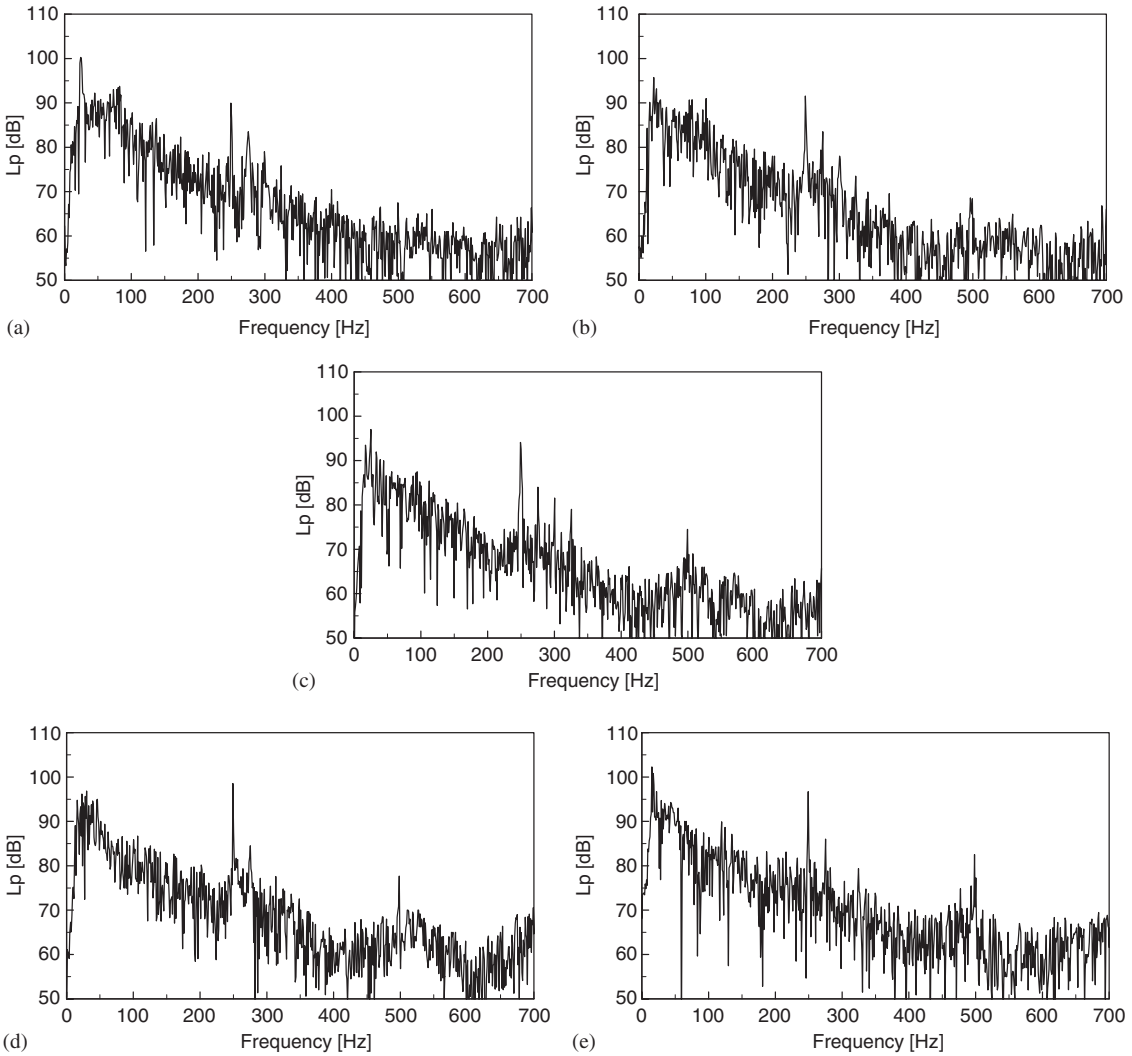

Fig. 6. Spectra of acoustic pressure levels (dB, Ref. 20 μPa) at the fan exit duct: (a) $Q = 0.40 \times$ BEP, (b) $Q = 0.75 \times$ BEP, (c) $Q =$ BEP, (d) $Q = 1.35 \times$ BEP, and (e) $Q = 1.70 \times$ BEP.

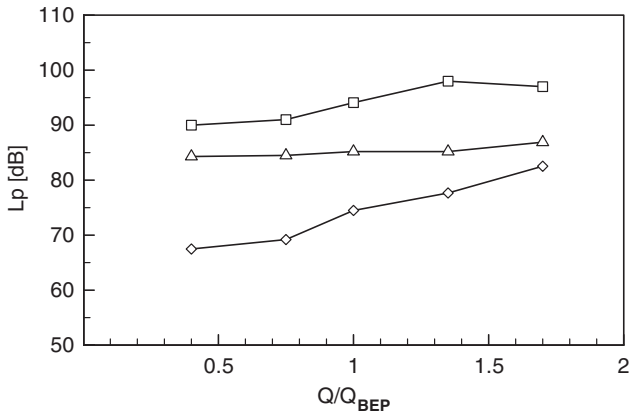

Fig. 7. Acoustic pressure levels (dB, Ref. 20 μPa) of the main tonal noise components at the fan exit duct: $f = 250$ Hz, BPF (white squares); $f = 275$ Hz (white triangles); $f = 500$ Hz, $2 \times$ BPF (white diamonds).

Table 2
Angular coordinates of the measurement points over the volute surface

Tongue points	Angular position (°)	Volute points	Angular position (°)	Volute points	Angular position (°)
P01	0	P06	60	P11	210
P02	2	P07	90	P12	240
P03	9	P08	120	P13	270
P04	16	P09	150	P14	300
P05	23	P10	180		

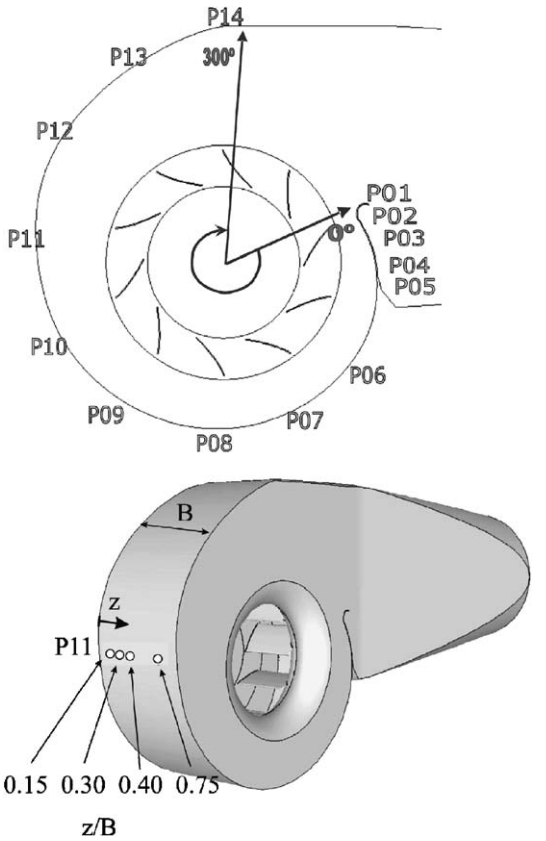

Fig. 8. Sketches of the fan with the measurement points.

Fig. 1. The origin of the angles is located at the volute tongue. In each angular position, four measurements have been made at the following z/B-coordinates (where B is the volute width): 0.15, 0.30, 0.40 and 0.75. The origin of z-coordinates is located at the impeller hub and $z/B = 0.54$ corresponds to the impeller shroud.

Figs. 9–11 represent the power spectra in dB (Ref. 20 μPa) of pressure fluctuations at the volute surface, measured at the BEP. The measurement positions selected and represented in these three figures are: P02 (at the volute tongue), P10 (at 180° from the tongue) and P14 (at 300° from the tongue, close to the outlet duct connection).

Important differences appear between the signals measured near the tongue (point P02) and those measured far from the tongue. At the tongue, the peak generated at the BPF is dominant, except in the position $z/B = 0.75$, placed near the volute front casing, at which the broad band noise is predominant. At the flow rates higher than BEP, the peak at the BPF increases strongly in this measurement position.

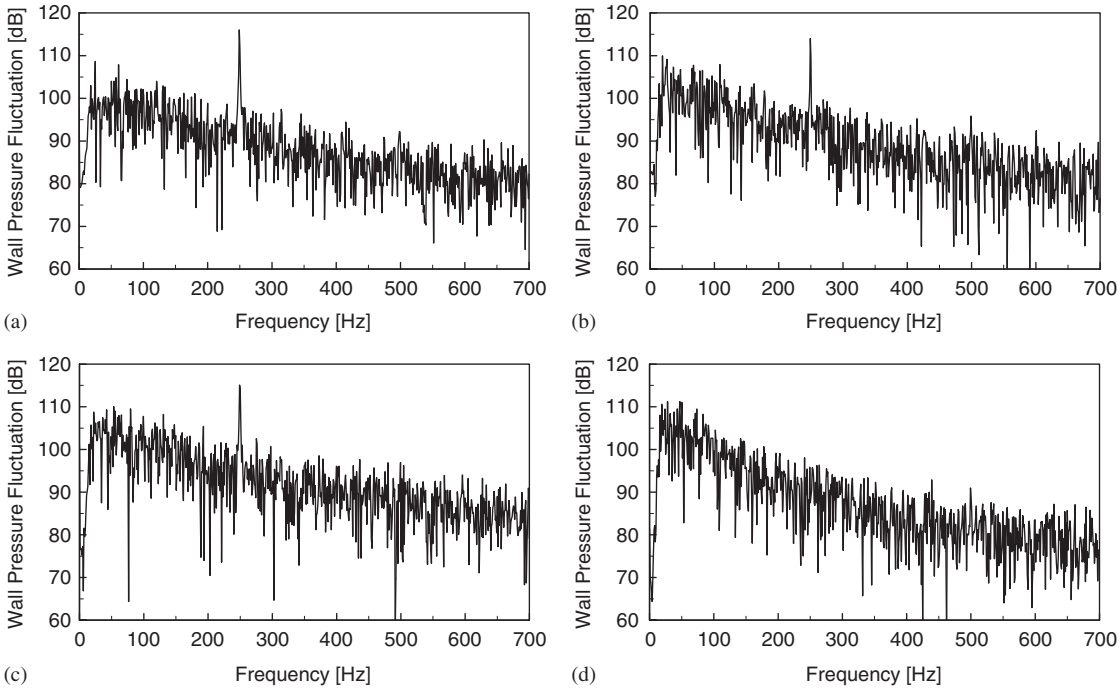

Fig. 9. Spectra of volute pressure fluctuations (dB, Ref. 20 μPa) at measurement point P02 (at the tongue), with the fan operating at the best efficiency point (BEP): (a) $z/B = 0.15$, (b) $z/B = 0.30$, (c) $z/B = 0.40$, and (d) $z/b = 0.75$.

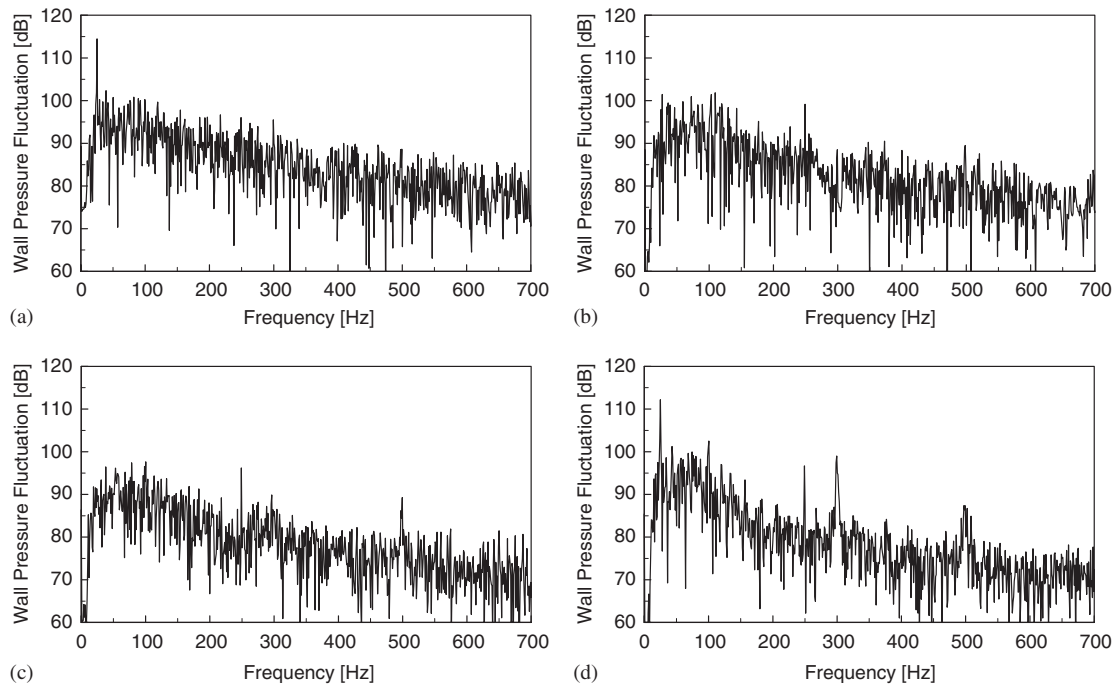

Fig. 10. Spectra of volute pressure fluctuations (dB, Ref. 20 μPa) at measurement point P10 (at 180° from the tongue), with the fan operating at the best efficiency point (BEP): (a) $z/B = 0.15$, (b) $z/B = 0.30$, (c) $z/B = 0.40$, and (d) $z/b = 0.75$.

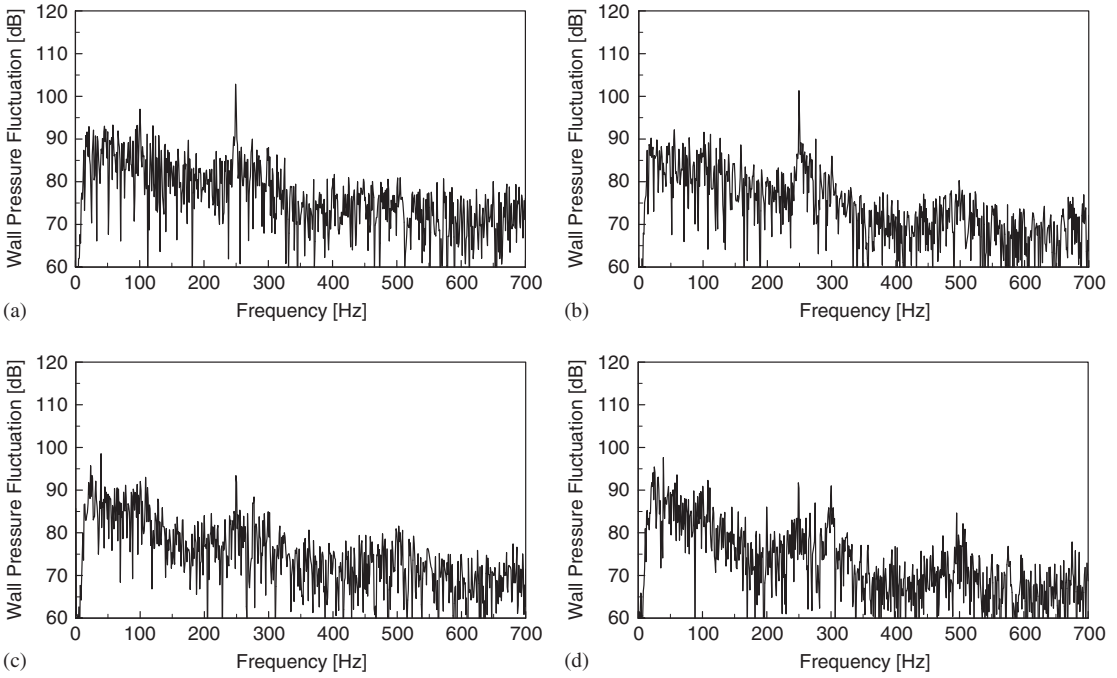

Fig. 11. Spectra of volute pressure fluctuations (dB, Ref. 20 μPa) at measurement point P14 (at 300° from the tongue, close to the outlet duct connection), with the fan operating at the best efficiency point (BEP): (a) $z/B = 0.15$, (b) $z/B = 0.30$, (c) $z/B = 0.40$, and (d) $z/b = 0.75$.

However, at points P10 and P14, some peaks at 275, 300 and 325 Hz appear besides the BPF at 250 Hz, suggesting the existence of mechanical sources of noise in accordance with the exit duct spectra shown above.

In addition, important broad band levels at low frequencies appear in all these spectra, independent from the flow rate and the measurement position changes. This pattern agrees with the sound pressure level spectra measured at the fan exit duct.

3.3. Vibration signals at the volute surface

In order to clarify the origin of the peaks observed at 275, 300 and 325 Hz, some vibration signals at the volute front casing were obtained with a 4384 B&K piezoelectric accelerometer, connected to a 2635 B&K amplifier. These signals were then transmitted to a 2133 B&K two-channel narrow-band frequency analyzer. Fig. 12 shows the spectra of these vibration signals at six angular positions on the front casing: at 0°, 60°, 120°, 180°, 240° and 300° from the tongue, i.e. the same angular positions as measurement points P01, P06, P08, P10, P12 and P14. These tests have been carried out under two operating conditions: with zero flow rate (named $Q = 0$ in the figure), and with the maximum flow rate analyzed in this study ($Q = 1.70 \times$ BEP in the figure).

In these spectra, a noticeable peak at the BPF is shown, increasing with the flow rate. Therefore, it is shown that the pressure fluctuations generated by the impeller flow generate some casing vibration. Also, important peaks at 275, 300 and 325 Hz appear in some cases. In particular, high vibration values at these frequencies have been measured placing the accelerometer in a zone of the front casing located between 120° and 240° with respect to the volute tongue. These values do not vary with the flow rate thus evidencing its mechanical origin. Moreover, an impact test demonstrated that the vibration signal at 300 Hz is due to a casing resonance caused by the excitation of a natural frequency.

These results show that components of the signals measured by the microphones at 275, 300 and 325 Hz correspond to mechanical vibrations measured by the accelerometers at the fan casing; the microphones have measured at these frequencies noise due to structural vibrations and not to pressure fluctuations generated by

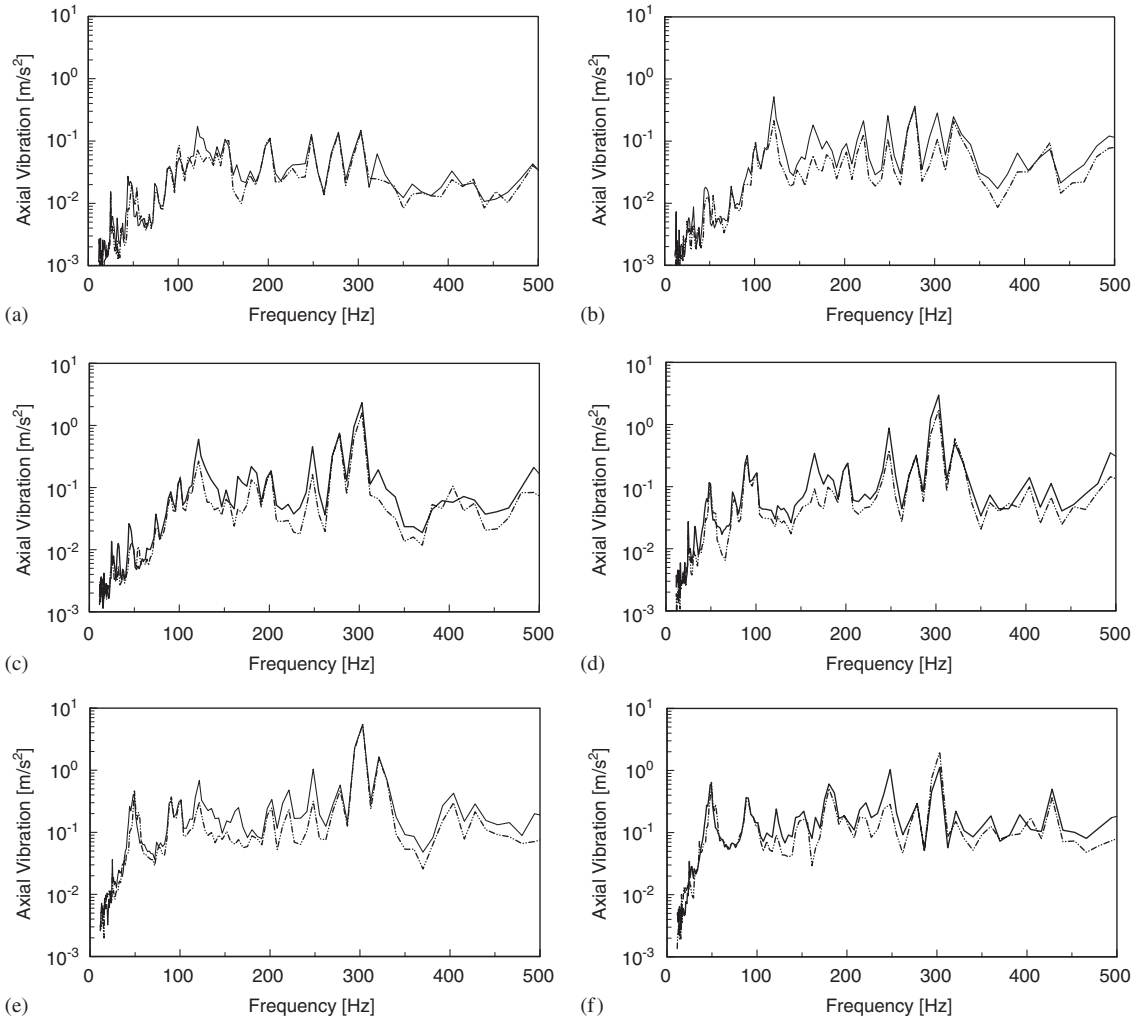

Fig. 12. Spectra of vibration signals (m/s^2) at the volute front casing, $Q = 0$ (dashed line) and $Q = 1.70 \times$ BEP (solid line): (a) angular position 0°; (b) angular position 60°; (c) angular position 120°; (d) angular position 180°; (e) angular position 240°; and (f) angular position 300°.

the impeller. Spectra of acoustic pressure obtained at the fan exit duct show that those components of the signals propagate effectively downstream of the fan, thus acting like a source of noise which contribution to the overall sound generation cannot be neglected.

3.4. Correlation analysis of BPF signals

In this section, a correlation method is applied in order to analyze the tonal noise generation at the BPF, determining the zone of effective acoustic radiation. If the interest is in the contribution of the pressure fluctuation on the volute surface to the sound pressure at the fan exit duct, independent of possible propagation paths and dispersion, an effective way for identifying energy sources is using the coherent output power in the frequency domain. The coherent power spectrum of volute pressure fluctuations has been calculated as follows:

$$\mathrm{CPS}\,(f) = \gamma^2\,(f)\mathrm{PS}\,(f). \tag{1}$$

Whereas the level (dB, Ref. 20 μPa) of CPS at the BPF has been then calculated as follows:

$$\mathrm{CPSL_{BPF}} = 20 \log \frac{\mathrm{CPS_{BPF}}}{p_0}. \tag{2}$$

Determination of the coherent part of a signal is discussed in more detail by Bendat and Piersol [15]. This method has been proven successfully in source identification of fan noise [10]. Fehse and Neise [14] investigated the generation mechanisms of broad band low-frequency noise in centrifugal fans. They found that the noise was caused by classical flow separation regions located on the impeller's shroud and the blade suction sides. Also the parts of the volute close to the impeller, specially the tongue area, were identified as a source region.

The first step is the calculation of the coherence function γ^2 between the volute pressure fluctuation and the acoustic pressure at the fan exit duct. Fig. 13 shows the spectra of coherence function γ^2, with the fan operating at the BEP, at two measurement points: P02 (at the tongue), and P14 (at 300° from the tongue, close to the outlet duct connection). At the tongue, the coherence function presents a value very close to the unity at the BPF. At the point placed near the outlet duct connection this value is slightly lower, but also close to the unity. At this measurement point, very high values of the coherence function at 275 and 300 Hz are also present. In order to assure the correlation between the two types of signals at the BPF, the phase angle of the cross spectrum has been calculated. If the two signals are correlated to each other, then the phase will be $2\pi f \Delta x/c$, where f is the frequency, Δx the physical separation distance between the two sensors and acoustic propagation at speed c is presumed. In Table 3, the values of coherence function γ^2 and phase angles (calculated and measured) at the measurement points P02 and P14 are presented. In general, a good correlation between the signals is observed at the flow rates close to the best efficiency one (0.75 × BEP, BEP and 1.35 × BEP), with coherence function values close to the unity and coincidence between the calculated and measured phase angles. With flow rates apart from the BEP (0.40 × BEP and 1.70 × BEP), the correlation between the signals is not so good.

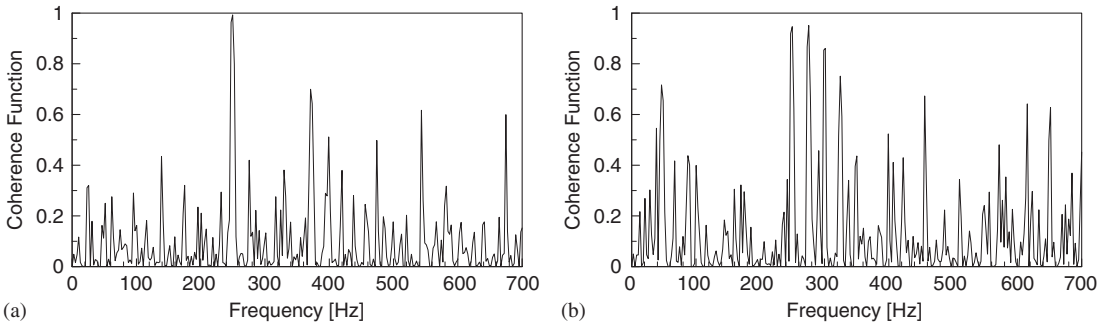

Fig. 13. Spectra of coherence function γ^2, with the fan operating at the best efficiency point (BEP), at two measurement points: (a) P02, at the tongue; and (b) P14, at 300° from the tongue, close to the outlet duct connection.

Table 3
Values of coherence function γ^2 and phase angles (calculated and measured) at the blade passing frequency, at two measurement points: P02 (at the tongue) and P14 (at 300° from the tongue, close to the outlet duct connection)

Flow rate	P02 (tongue)			P14 (outlet duct)		
	Coherence function	Phase angle (calculated)	Phase angle (measured)	Coherence function	Phase angle (calculated)	Phase angle (measured)
0.40 × BEP	0.81	−48	−96	0.92	164	157
0.75 × BEP	0.94	−48	−44	0.90	164	117
BEP	0.98	−48	−48	0.94	164	169
1.35 × BEP	0.96	−48	−52	0.96	164	178
1.70 × BEP	0.83	−48	−11	0.70	164	−128

The following step is the calculation of the coherent levels at the BPF for all the measurement points on the volute. In Fig. 14, the coherent levels at the BPF, $CPSL_{BPF}$ (dB, Ref. 20 μPa), have been represented on the volute surface. The z-coordinate has been divided by the volute width B (248 mm). The impeller shroud corresponds to $z/B = 0.54$, $z/B = 0$ is the volute rear casing and $z/B = 1$ is the volute front casing.

From a detailed analysis of Fig. 14 we can identify, in a qualitative way, the main mechanisms of aerodynamic tonal noise generation, and its flow rate dependence. According to Neise [4], the primary causes of aerodynamic fan noise are the unsteady forces on the blades and the casing generated by their interaction with the turbulent flow. The unsteady forces on the blades are generated by a spatially non-uniform flow field, pressure fluctuations in the turbulent blade boundary layer, vortex separation from the blades and secondary flows. The acoustic efficiency of the unsteady forces on the blades is high, and hence, they represent an important contribution to the radiated fan noise. Additionally, unsteady forces are also exerted on stationary parts of the fan. In the case of centrifugal fans, the unsteady flow leaving the rotating impeller channels generates pressure fluctuations of high amplitude at the volute tongue which is regarded as the main source region of the aerodynamic tonal noise for these fans.

Next, with respect to Fig. 14, we describe the two main mechanisms of aerodynamic tonal noise generation found in this fan: unsteady forces exerted on the impeller blades and those exerted on the volute tongue. The latter mechanism will be described first, as it becomes predominant.

(i) Unsteady forces exerted on the volute tongue

In all the cases studied, this noise mechanism is predominant: a strong source of noise caused by the interaction between the fluctuating flow leaving the impeller and the volute tongue is appreciated. This noise source is revealed by very high levels of the coherent level concentrated in a small region in the vicinity of the volute tongue. The position and extension of this interaction region and the magnitude of the corresponding levels strongly depend on the flow rate. In order to appreciate clearly the interaction region for each flow rate, a different range of amplitudes has been used for the flow rates: $0.4 \times$ BEP, $0.75 \times$ BEP and BEP, than for the flow rates $1.35 \times$ BEP and $1.70 \times$ BEP. In this way, the highest levels appear in red in all the cases and this fact permitted us to qualitatively identify the position of this noise source.

For all the flow rates analyzed, these highest values, associated to the flow-volute tongue interaction, appear only in the volute width corresponding to the impeller width. Outside the impeller width, i.e. for volute positions with z/B greater than 0.54, the coherent levels remain almost constant in the angular direction, revealing no influence from the volute tongue.

For the lowest flow rate analyzed, i.e. $0.4 \times$ BEP, the highest levels of the coherent level do not appear precisely in the volute tongue but 20° away (always towards the interior of the volute). When the flow rate increases ($0.75 \times$ BEP), the highest levels present similar values as in the previous flow rate but they appear 10° away from the volute tongue. For the BEP, the highest levels of the coherent level increase with respect to the previous flow rates and they appear very close to the volute tongue. For flow rates higher than BEP ($1.35 \times$ BEP and $1.70 \times$ BEP), the highest levels of the coherent level increase with respect to the previous flow rate and they appear precisely in the volute tongue.

The high coherent levels found at the volute tongue for the flow rate corresponding to the BEP are noteworthy. They reveal a deficient fan design in order to minimizing the interaction between the impeller and the volute. In a correctly designed radial turbomachine, no impingement must exist between the volute tongue and the flow leaving the impeller at the flow rate corresponding to the BEP. Thus, for that flow rate (BEP), small pressure fluctuations are usually expected at the volute tongue, and then a reduced influence of this mechanism of noise generation. This deficient coupling is probably due to the fact that the manufacturer usually supplies the same volute with different interchangeable impellers, in order to produce different working conditions. Thus, we believe that the volute is not optimized for the impeller tested.

(ii) Unsteady forces exerted on the fan blades

The unsteady forces exerted on the fan blades constitute another noise generation mechanism, which affects the whole extension of the impeller, thus transmitting pressure fluctuations to all the measurement locations over the volute casing. The relative importance of this mechanism compared to the interaction

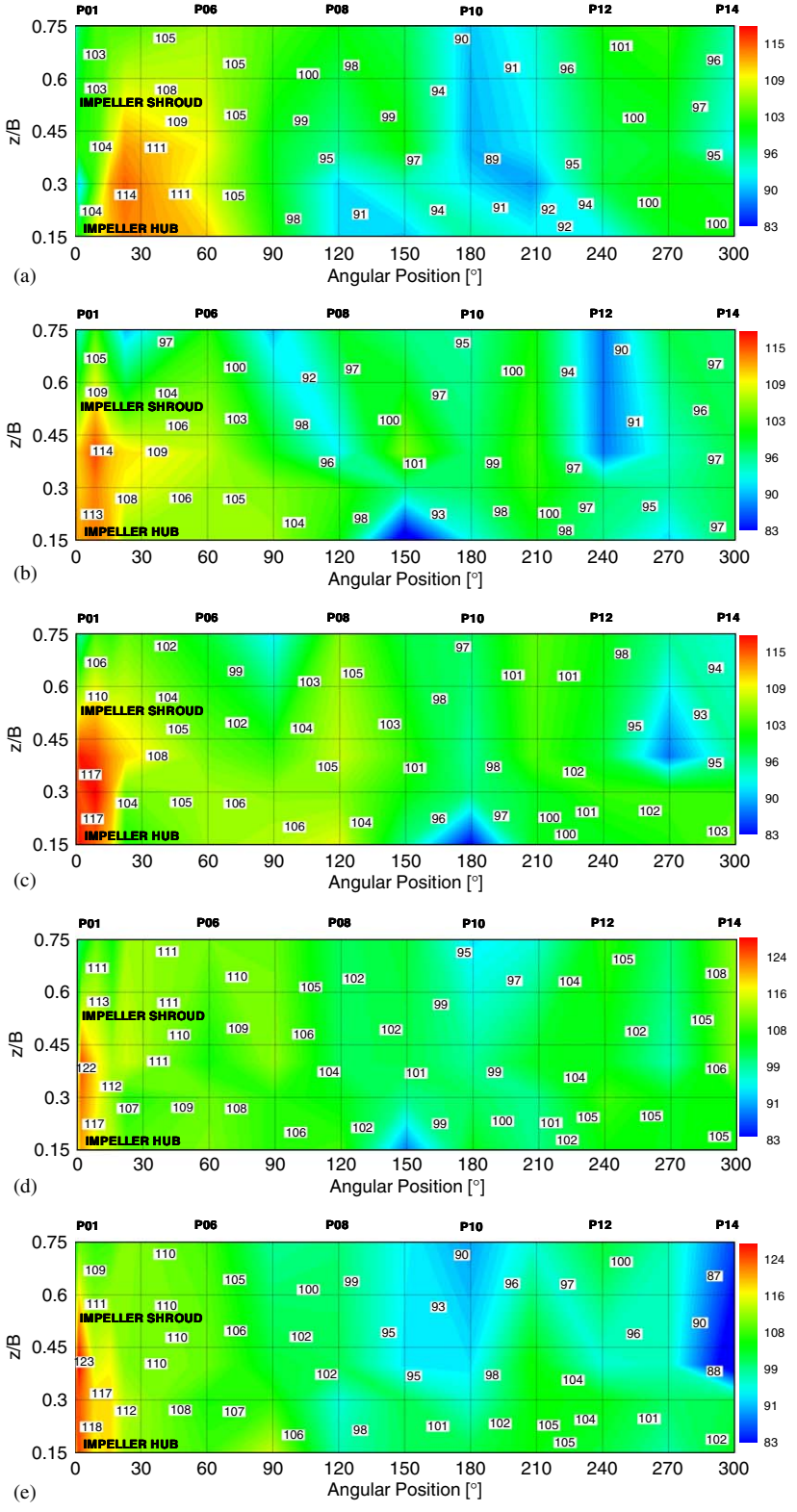

Fig. 14. Coherent levels at the blade passing frequency $CPSL_{BPF}$ (dB, Ref. 20 μPa), calculated by correlation of wall pressure sensors and the microphone at the fan exit duct: (a) $Q = 0.40 \times$ BEP, (b) $Q = 0.75 \times$ BEP, (c) $Q =$ BEP, (d) $Q = 1.35 \times$ BEP, and (e) $Q = 1.70 \times$ BEP.

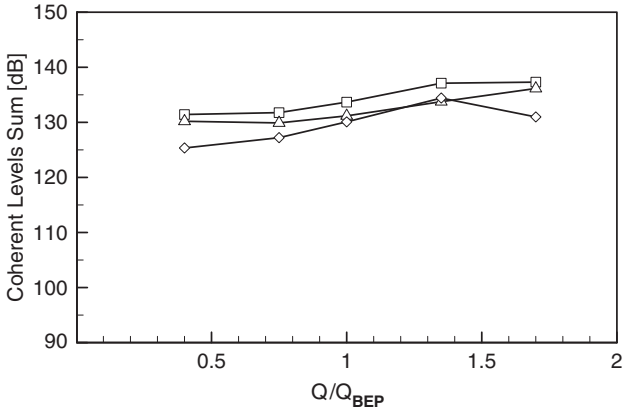

Fig. 15. Area-weighted sums of the coherent levels at the blade passing frequency (dB, Ref. 20 μPa), overall (white squares) and split into two zones: close to the volute tongue (white triangles) and in the rest of the volute (white diamonds).

forces exerted on the volute tongue also depends on the flow rate. For the flow rates near the BEP ($0.70 \times$ BEP, BEP and $1.35 \times$ BEP) the coherent levels outside the volute tongue zone are significant, suggesting a notable influence of the unsteady forces on the blades in the total noise generation. However, for flow rates distant from the BEP ($0.40 \times$ BEP and $1.70 \times$ BEP) very high coherent levels appear only concentrated in the vicinity of the volute tongue, whereas in the rest of the volute the coherent levels are very low, thus suggesting that for these flow rates, the interaction unsteady forces on the volute tongue constitute the only noise generation mechanism.

These arguments are outlined in Fig. 15, in which an area-weighted summation of the coherent levels shown in Fig. 14 is presented, for different flow rates. The overall values of this summation have been split into two areas: a zone close to the volute tongue (between 0° and 60°) and the rest of the volute (between 60° and 300°).

The analysis of the coherent levels sums shown in Fig. 15 explains why the highest outlet duct noise level at the BPF appears at $1.35 \times$ BEP, and then even slightly decreases (see the tendency shown in Fig. 7). If only the contribution of the interaction between the impeller and the volute tongue were taken into account, the acoustic pressure at the fan exit duct should increase continuously with the flow rate, according to the line made up of triangles in Fig. 15. In this fan, on the contrary, the highest value of the acoustic pressure at the fan exit duct coincides with high coherent levels both in the volute tongue and the rest of the volute, and this happens in a specified operation zone (around $1.35 \times$ BEP) in which both noise generation mechanisms (i) and (ii) are very effective: the lines made up of triangles and diamonds in Fig. 15 are concurrent at $1.35 \times$ BEP. Above this flow rate, the acoustic pressure at the fan exit duct at the BPF does not increase because only mechanism (i) is efficient. As a result of the features explained, the overall values of the coherent levels sums (line made up of squares in Fig. 15) present a trend very similar to that shown in Fig. 7 for the acoustic pressure levels at the fan exit duct.

As was stated above, mechanism (i) is usually referred as the dominant in centrifugal fans, and it is the main focus of research into fan noise generation. But in this fan, a different behavior has been detected, with relevant contributions in other regions of the volute. The reason for this sound generation pattern could derive from the relatively great distance between the impeller and the volute tongue in this fan.

Due to the features explained above, we think that a prediction method of the tonal noise generation in this fan should include the whole impeller–volute arrangement and not only the region in the vicinity of the volute tongue.

4. Conclusions

The sound pressure level spectra measured at the fan exit duct exhibit important broadband and peak contributions related to mechanical sources besides the aerodynamic tonal noise at blade passing frequency.

The peak at the blade passing frequency appears clearly in all the flow rates studied. This component increases with the flow rate until $1.35 \times$ BEP, and above this operating point the blade passing frequency decreases slightly. The first harmonic at 500 Hz increases with the flow rate over all the operating range, but its values are very low; at low flow rates, it is practically masked by the broad band noise at adjacent frequencies.

Regarding the pressure fluctuations at the volute surface, important differences appear between the signals measured near the tongue and those measured far away from the tongue. At the tongue, the peak generated at the blade passing frequency is dominant, except in the position $z/B = 0.75$, near the front casing, in which the broad band noise is predominant. At the flow rates higher than BEP, the peak at the blade passing frequency increases strongly in this measurement zone. At the measurement positions far away from the tongue, some peaks not related to aerodynamic phenomena appear besides the blade passing frequency with noticeable amplitudes. In addition, important broad band levels at low frequencies appear in all these spectra, independently from the flow rate and measurement position changes.

Vibration signals obtained at the volute front casing show that at 275, 300 and 325 Hz, the microphones have measured noise due to mechanical vibrations and not to pressure fluctuations generated by the impeller flow. Spectra of acoustic pressure obtained at the fan exit duct show that those components of the signals propagate effectively downstream of the fan, thus acting like a source of noise whose contribution to the overall sound generation cannot be neglected.

In all the cases studied, a strong source of noise caused by the interaction between the fluctuating flow leaving the impeller and the volute tongue is appreciable. The unsteady forces exerted on the fan blades constitute another noise generation mechanism, which affects the whole extension of the impeller, thus transmitting pressure fluctuations to the entire volute casing. In this fan, the highest values of the acoustic pressure at the fan exit duct appear in a specified operation zone (around $1.35 \times$ BEP) in which both aerodynamic tonal noise generation mechanisms are very effective.

The results described in this paper contribute to explaining the noise generation sources in this kind of centrifugal fans and will be very helpful in the implementation and validation of prediction codes for aerodynamic tonal noise generation.

Acknowledgments

This work was supported by the Research Projects TRA2004-4269 and DPI2001-2598 (Ministry of Science and Technology, Spain).

References

[1] M.J. Lighthill, On sound generated aerodynamically. I. General theory, *Proceedings of the Royal Society A* 211 (1952) 564–587.
[2] A. Powell, Theory of vortex sound, *Journal of the Acoustical Society of America* 16 (1964) 177–194.
[3] J.E. Ffowcs Williams, D.L. Hawkings, Sound generation by turbulence and surfaces in arbitrary motion, *Philosophical Transactions of the Royal Society A* 264 (1969) 321–342.
[4] W. Neise, Review of fan noise generation mechanisms and control methods, *Proceedings of FAN NOISE Symposium*, Senlis, September 1992.
[5] S. Chu, R. Dong, J. Katz, Relationship between unsteady flow, pressure fluctuations, and noise in a centrifugal pump—part B: effects of blade–tongue interactions, *ASME Journal of Fluids Engineering* 117 (1995) 30–35.
[6] Y. Ohta, E. Outa, K. Tajima, Evaluation and prediction of blade-passing frequency noise generated by a centrifugal blower, *ASME Journal of Turbomachinery* 118 (1996) 597–605.
[7] Y. Ohta, M. Hikichi, E. Outa, K. Tajima, S. Saito, Active cancellation of noise sources in a centrifugal blower, *Proceedings of Ninth International Symposium on Unsteady Aerodynamics Aeroacoustics and Aeroelasticity of Turbomachines*, Lyon, September 2000, pp. 182–193.
[8] M.C. Thompson, K. Hourigan, Prediction of the noise generation in a centrifugal fan by solution of the acoustic wave equation, *Proceedings of the FAN NOISE Symposium*, Senlis, September 1992, pp. 197–204.
[9] I.C. Shepherd, R.F. Lafontaine, Measurement of vorticity noise sources in a centrifugal fan, *Proceedings of the FAN NOISE Symposium,* Senlis, September 1992, pp. 205–212.
[10] Th.H. Carolus, M. Stremel, Blade surface pressure fluctuations and acoustic radiation from an axial fan rotor due to turbulent inflow, *Acta Acustica United with Acustica* 88 (2002) 472–482.
[11] International Organization for Standardization ISO 5136: 2003. Determination of sound power radiated into a duct by fans and other air-moving devices. In-duct method.

[12] S. Velarde-Suárez, C. Santolaria-Morros, R. Ballesteros-Tajadura, Experimental study on the aeroacoustic behavior of a forward-curved centrifugal fan, *ASME Journal of Fluids Engineering* 121 (1999) 276–281.
[13] S. Velarde-Suárez, R. Ballesteros-Tajadura, C. Santolaria-Morros, J. González-Pérez, Unsteady flow pattern characteristics downstream of a forward-curved blades centrifugal fan, *ASME Journal of Fluids Engineering* 123 (2001) 265–270.
[14] K.R. Fehse, W. Neise, Generation mechanisms of low-frequency centrifugal fan noise, *AIAA Journal* 37 (1999) 1173–1179.
[15] J.S. Bendat, G. Piersol, *Engineering Applications of Correlation and Spectral Analysis*, Wiley, New York, 1980.